33RD INTERNATIONAL COSMIC RAY CONFERENCE, RIO DE JANEIRO 2013
THE ASTROPARTICLE PHYSICS CONFERENCE

ICRC 2013

Seasonal variation of atmospheric neutrinos in IceCube

THE ICECUBE COLLABORATION[1]

[1]*See special section in these proceedings*

desiati@wipac.wisc.edu

Abstract: The IceCube Observatory is a cubic-kilometer neutrino telescope at the South Pole, which currently collects about 170 well-reconstructed neutrinos per day with energies above 100 GeV. These neutrinos are generated by cosmic ray interactions in the atmosphere, and their rate is expected to correlate with the atmospheric density, which depends on the temperature. A large portion of upward moving neutrinos reconstructed within 30° of the horizon is produced above the Antarctic continent. This component of the upward neutrino flux is therefore expected to correlate with the stratospheric temperature in a similar way as downward-going muons produced in the atmosphere above IceCube. We report the first observation of an annual modulation of the atmospheric neutrino flux in correlation with the upper atmospheric temperature. Its amplitude of about ±5% is inconsistent with a constant rate at a confidence level of 3.4 sigma.

Corresponding authors: P. Desiati[1], K. Jagielski[2], A. Schukraft[2], G.C. Hill[3], T. Kuwabara[4], T. Gaisser[4]
[1]*Wisconsin IceCube Particle Astrophysics Center, University of Wisconsin, Madison, WI 53706, U.S.A.*
[2]*III. Physikalisches Institut, RWTH Aachen University, 52056 Aachen, Germany*
[3]*School of Chemistry and Physics, University of Adelaide, Australia*
[4]*Bartol Research Institute and Dept. of Physics and Astronomy, University of Delaware, Newark, DE 19716, U.S.A.*

Keywords: cosmic rays, neutrinos, seasonal modulation, IceCube

1 Introduction

Understanding the lepton flux produced by the interaction of cosmic rays with the Earth's atmosphere is important for neutrino observatories. These events are the main sources of background in the search for astrophysical neutrinos, and they are also important for calibrating the detector. In addition, the fluxes of atmospheric muons and neutrinos provide an indirect probe of the particle physics of hadronic showers in the atmosphere.

The correlation of the lepton fluxes with temperature in the upper atmosphere is an interesting detail to study, in part because the general features of the normalization (such as the primary spectrum) cancel to a large extent. Pions and kaons produced by interactions of cosmic rays either interact again or decay into muons and neutrinos. The competition between the two processes depends on the local density of the atmosphere in the production region, which changes with temperature [1]. The correlation of the intense muon flux with the upper atmospheric temperature has been extensively studied by various experiments at different energy thresholds [2, 3, 4, 5]. The IceCube Observatory provides observations with unprecedented statistics that show correlations on short time scales with variations in the stratosphere over Antarctica [6] as well as the yearly modulation of the muon flux [7]. Study of seasonal variations can provide a constraint on the kaon to pion production ratio in the extensive air showers [8, 7], and is also a tool to probe charm production [9].

With the kilometer-scale IceCube Observatory it is possible for the first time to obtain enough events to observe the correlation of the neutrino flux with the upper atmospheric temperature. A similar study done with the smaller AMANDA detector [10] lacked the statistics to demonstrate the expected correlation. In this paper we present a correlation study of the atmospheric neutrino flux with the stratospheric temperature, along with the theoretical expectations.

2 Neutrino and Temperature Data

IceCube consists of 5160 optical sensors viewing a cubic kilometer of ice at a depth of 1450 to 2450 meters in the Antarctic glacier (see [11] for an overview of IceCube). This study uses about 90,000 neutrino-induced, upward muon events collected by IceCube in 1040 days of operation, from April 2008 to May 2011. During this period IceCube was under construction, and the instrumented volume increased from 40 deployed strings in 2008 (IC40) to 59 strings in 2009 (IC59) and 79 in 2010 (IC79). The neutrino event samples summarized in Table 1

configuration	time period	events	livetime
IC40 (40 strings)	4/2008 - 5/2009	12877	375.5 d
IC59 (59 strings)	5/2009 - 5/2010	21943	348.1 d
IC79 (79 strings)	6/2010 - 5/2011	54999	315.5 d

Table 1: Neutrino event samples selected from the three detector configurations considered in this analysis, with data collection time period, number of selected events and the corresponding livetime (in days) [12, 13, 14].

were selected by independent data analyses to determine their energy spectrum [12] or to search for neutrinos of extra-terrestrial origin [13, 14]. In these data samples, muon neutrino induced events were separated from the

large background of atmospheric muons from above by selecting well reconstructed upward-going tracks. Most of the neutrino events are of atmospheric origin. Their flux is therefore correlated with the temperature variations in the atmosphere where they were produced. The contamination of mis-reconstructed atmospheric muon events is less than 1%.

For the purpose of studying correlation with temperature in the upper atmosphere where the neutrinos are produced, it is convenient to divide the hemisphere below the detector into three zones. Zone 1 contains events with zenith angles in the range $90^\circ < \theta < 120^\circ$, which covers a solid angle of π sr corresponding to latitudes between -30° and -90°. Zone 2 ($120^\circ < \theta < 150^\circ$), with a solid angle of 0.73π corresponds to the equatorial region with latitudes in the range $\pm 30^\circ$. Zone 3 ($150^\circ < \theta < 90^\circ$) covers the Northern temperate latitudes and the Arctic region. The total solid angle of Zone 3 as seen from the South Pole is small (0.27π sr), and the Arctic region is only 15% of this. The seasonal temperature variation in the equatorial zone is small, so it is not suited for measuring correlation with variations in temperature. Zone 1 has half the total solid angle and contains more than half the neutrino-induced muons because the high-energy atmospheric neutrino flux is largest near the horizon. The temperature variation in Zone 1 has the same phase as that at the South Pole, and about 35% of this region is over the Antarctic continent. In this paper only neutrino events in Zone 1 are considered.

3 Temperature Correlation

The relevant temperatures and densities are those where the neutrinos are produced. It is therefore necessary to convolve the temperature profile with the muon production spectrum along each direction considered. A simple analytic approximation for neutrino production is used to obtain a single effective temperature for each direction at each time.

In this approach [9], the differential flux of $\nu_\mu + \bar{\nu}_\mu$ is approximated as

$$\phi_\nu(E_\nu,\theta) = \phi_N(E_\nu) \times \left\{ \frac{A_{\pi\nu}}{1 + B_{\pi\nu}\cos\theta^\star E_\nu/\varepsilon_\pi} + \frac{A_{K\nu}}{1 + B_{K\nu}\cos\theta^\star E_\nu/\varepsilon_K} \right\}, \quad (1)$$

where $\phi_N(E_\nu)$ is the primary spectrum of nucleons (N) evaluated at the energy of the neutrino. The first term in Eq. 1 corresponds to neutrino production from leptonic and semi-leptonic decays of pions, while the second term is related to kaons. The constants $A_{\pi\nu}$ and $A_{K\nu}$ depend on the branching ratio for meson decay into neutrinos, the spectrum weighted moments of the cross section for a nucleon to produce secondary mesons, and those of the meson decay distribution. The denominators in Eq. 1 reflect the competition between decay and interaction of secondary mesons in the atmosphere. At energies below $\varepsilon_{\pi,K}/\cos\theta^\star$ (with the neutrino zenith angle evaluated at its point of production) meson decay is the dominant process, and neutrinos are produced with the same spectral index as the parent cosmic rays. At high energies meson interaction dominates and the corresponding neutrino spectrum becomes asymptotically one power steeper than the primary spectrum.

The characteristic critical energies $\varepsilon_{\pi,K}$ at a given atmospheric depth are inversely proportional to the atmospheric density at that point, and therefore are affected by temperature variations. In an isothermal approximation of the atmosphere, the density profile is described by an exponential with a scale height of $h_0 \sim 6.19$ km (over Antarctica). This numerical value corresponds to the lower stratosphere, where most of the neutrinos are generated. In the ideal gas law approximation, $\varepsilon_{\pi,K}$ are proportional to the atmospheric temperature in the isothermal approximation. At a mean atmospheric temperature of $T_0 = 224$ K (average over Zone 1) the critical energies are $\varepsilon_\pi = 117$ GeV and $\varepsilon_K = 871$ GeV. At energies far above $\varepsilon_{\pi,K}$, the terms in Eq. 1 reach the asymptotic regime where the flux is proportional to the mesons critical energy and, therefore, to the atmospheric temperature. This dependency is the source of the seasonal modulation of the neutrino flux.

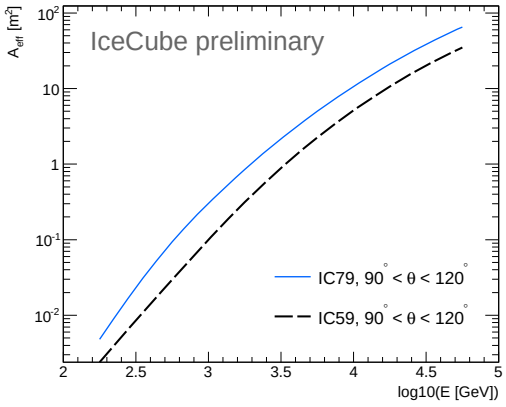

Fig. 1: Neutrino effective area, averaged over ν_μ and $\bar{\nu}_\mu$ as a function of neutrino energy (at the interaction point) for the sample selected with the 79-string detector configuration [14] (blue continuous line) and for the sample selected with the 59-string detector configuration [13] (black dashed line). The effective areas are averaged over the zenith angle ranges $90^\circ < \theta < 120^\circ$.

The effective temperature is the convolution of the actual atmospheric temperature profile over the atmospheric slant depth X (in g/cm^2) with the neutrino production spectrum profile $P_\nu(E_\nu,\theta,X)$, where critical energies are evaluated at the actual temperature at atmospheric depth X [7, 9]. Taking into account the detector response, the effective temperature is given by

$$T_{\rm eff}(\theta) = \frac{\int dE_\nu \int dX\, P_\nu(E_\nu,\theta,X) A_{\rm eff}(E_\nu,\theta)\, T(X)}{\int dE_\nu \int dX\, P_\nu(E_\nu,\theta,X) A_{\rm eff}(E_\nu,\theta)}, \quad (2)$$

where $A_{\rm eff}(E_\nu,\theta)$ is the neutrino effective area obtained from simulation which contains the detector acceptance, event selection, and the neutrino interaction cross section. The denominator in Eq. 2 is the total measured neutrino intensity. The total effective temperature $T_{\rm eff}$ is the weighted average of Eq. 2 over the actual zenith distribution of the neutrino-induced events.

Figure 1 shows the neutrino effective area for the IC59 and IC79 detector configurations for Zone 1. The selected neutrino events have a mean energy of the order of 1 TeV, therefore the high energy behavior of the effective area is not relevant for this analysis. Figure 1 shows that the events in the IC79 sample have a lower energy threshold than those in the IC59 sample. Because α_T^{th} increases with increasing

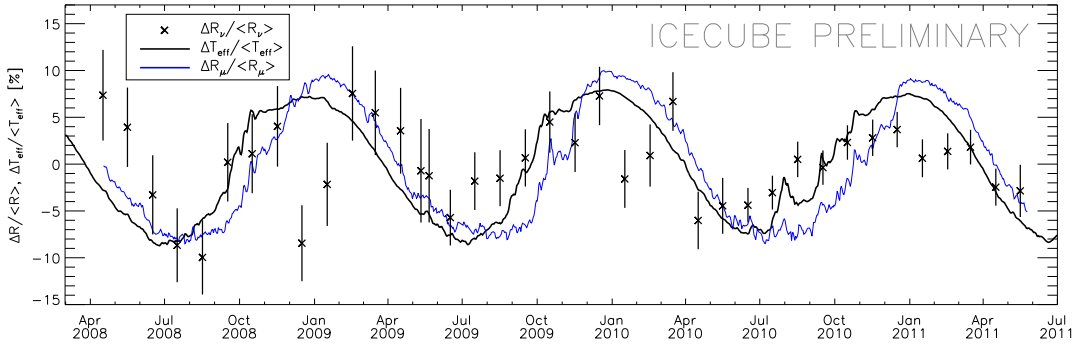

Fig. 2: The relative modulation of the effective temperature calculated for neutrinos collected within the zenith angle range $90^\circ < \theta < 120^\circ$ between April 2008 and July 2011 (black line), compared with the corresponding relative variation in the monthly neutrino rate (points with statistical errors). The blue line shows the downward muon event rate collected in the same time period. The statistical errors in the muon rates are small and not visible. The modulation of the nearly horizontal upward neutrinos is somewhat ahead of that for muons (see text).

energy threshold, the correlation analysis was performed separately for each event sample.

The atmospheric temperature profile data used in this analysis were collected by the NASA Atmospheric Infrared Sounder (AIRS) on board the Aqua satellite. Daily atmospheric temperatures at 24 different pressure levels from 1 to 1000 hPa at geographic locations around the globe were obtained from the AIRS Level 3 Daily Gridded Product available on NASA Goddard Earth Sciences, Data and Information Services Center (GES DISC) [15]. Using these data the daily effective temperature $T_{\rm eff}$ was calculated based on the zenith-weighted average of Eq. 2.

As with the muon case [7, 9], the relation between the variation of temperature and the variation of neutrino intensity at a given energy and zenith angle can be expressed in terms of a theoretical correlation coefficient calculated from Eq. 1 as [7]

$$\alpha_\nu(E_\nu,\theta) = \frac{T}{\phi_\nu(E_\nu,\theta)}\frac{\partial\phi_\nu(E_\nu,\theta)}{\partial T}, \qquad (3)$$

which depends explicitly on the characteristic critical energies $\varepsilon_{\pi,K}$. With increasing energy, the temperature correlation coefficient increases until it reaches a constant value at sufficiently high energy.

To compare the prediction with measurements, it is necessary to convolve the neutrino differential spectrum with the detector response. The corresponding weighted correlation coefficient is

$$\alpha_T^{th}(\theta) = \frac{T\cdot\frac{\partial}{\partial T}\int dE_\nu\,\phi_\nu(E_\nu,\theta)A_{\rm eff}(E_\nu,\theta)}{\int dE_\nu\,\phi_\nu(E_\nu,\theta)A_{\rm eff}(E_\nu,\theta)}. \qquad (4)$$

This equation defines the correlation coefficient for a particular zenith angle θ. The total correlation coefficient is then obtained by averaging $\alpha_T^{th}(\theta)$ over θ with a weight given by the observed event angular distribution. With this definition the relative variation in neutrino intensity I_ν is given by

$$\frac{\Delta I_\nu}{I_\nu} = \alpha_T^{th}\frac{\Delta T_{\rm eff}}{T_{\rm eff}}. \qquad (5)$$

Since the rate R_ν of observed neutrinos is proportional to the incident neutrino intensity I_ν, it is correlated with the effective temperature as well

$$\frac{\Delta R_\nu}{\langle R_\nu\rangle} = \alpha_T^{exp}\frac{\Delta T_{\rm eff}}{\langle T_{\rm eff}\rangle}, \qquad (6)$$

where α_T^{exp} is the experimentally determined correlation coefficient.

4 Results

Figure 2 shows the monthly rates of neutrino events with $90^\circ < \theta < 120^\circ$ relative to the mean annual rate, along with the corresponding effective temperatures relative to the mean. The monthly rate is calculated as the number of events divided by livetime in the corresponding month. The effective temperature is calculated with Eq. 2 using the neutrino effective area corresponding to each detector configuration. A yearly modulation of the neutrino rate is clearly observed, and a χ^2 analysis with the three years of IceCube data rejects a constant rate of neutrinos at the 3.4σ level. The apparently reduced rates during the months of January and February (when Antarctic summer operations occurred during construction) are under investigation. Figure 2 shows that the modulation in neutrino rate is correlated with the variation of the effective temperature. To quantify this correlation, a linear fit is performed, as shown in Fig. 3. The results are shown in Table 2. The decrease of the uncertainty in the correlation coefficient from IC40 to IC79 reflects the larger event samples collected with the bigger instrumented volume. As mentioned, the temperature correlation coefficient was not determined by stacking the three data samples because of their different energy thresholds.

configuration	α_T^{exp}	χ^2/ndf	α_T^{th}
IC40	0.27 ± 0.21	22.85/12	$0.557^{+0.008}_{-0.007}$
IC59	0.50 ± 0.15	12.30/11	$0.518^{+0.008}_{-0.007}$
IC79	0.45 ± 0.11	4.48/10	$0.489^{+0.007}_{-0.005}$

Table 2: Experimental and theoretical neutrino temperature correlation coefficients corresponding to the three detector configurations and the χ^2/ndf of for the experimental coefficient. Errors on α_T^{exp} are statistical and those on α_T^{th} are from the seasonal change of critical energies $\varepsilon_{\pi,K}$.

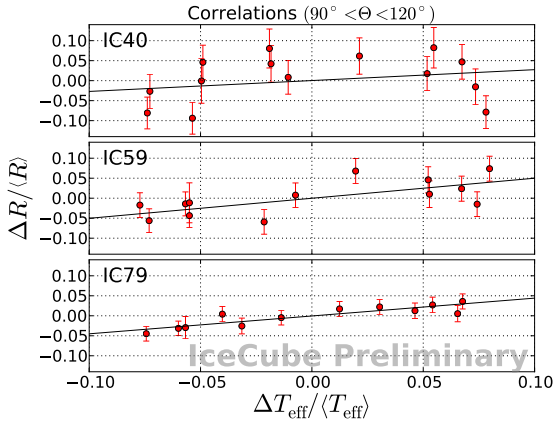

Fig. 3: Correlation between the the measured monthly relative rate variation and that of the corresponding effective temperature for the three detector configurations datasets for $90^\circ < \theta < 120^\circ$. The linear fits are also shown and the results shown in Table 2.

Systematic uncertainties of the analysis arise from understanding of the detector (light yield, ice properties, efficiency of the optical sensors) and from uncertainties in the theoretical parameters such as the spectral index and the K/π ratio. The latter is particularly important because the charged kaon channel is the main source of muon neutrinos above 100 GeV. For both sources of experimental error, however, the effects are relatively small because the same uncertainties occur in the numerator and the denominator of key quantities such as $T_{\rm eff}$ (Eq. 2) and the correlation coefficient, Eq. 4.

One of the main experimental uncertainties is the optical sensitivity of the detector, which includes e.g. the photon light yield of propagating particles in the ice, efficiency of IceCube's optical sensors and the global transparency of the ice. A 20% uncertainty on this parameter results in a variation of α_T^{exp} of less than $\pm 1\%$ and a variation of α_T^{th} of $\pm 4\%$.

Events in Zone 1 ($90^\circ < \theta < 120^\circ$) are produced in the southern atmosphere so their correlation with temperature is expected to be similar to that of the downward cosmic ray induced muons [7] produced locally in the atmosphere above the detector. The apparent difference in phase between the muons and neutrinos in Fig. 2 is likely due to the fact that at more horizontal directions the pions and kaons decay higher in the atmosphere, making the peak of neutrino production spectrum shift to smaller atmospheric depths. Since the atmospheric temperature increases sooner in the upper atmosphere than in the lower layers when the Sun rises in the austral spring, the modulation of the horizontal neutrino flux would be expected to precede that of the more vertical downward muons. At the same time, temperature modulations are larger at higher altitudes. This makes the variation in $T_{\rm eff}$ for neutrinos comparable to that for muons even though neutrinos are produced in more temperate latitudes within Zone 1.

The differential flux of muons is represented by an expression similar to Eq. 1 at sufficiently high energy (>100 GeV). However, the fractional contributions of the main hadronic channels to the production of leptons in the atmosphere are different for muons and neutrinos. The kinematics of $\pi^\pm \to \mu^\pm + \nu$ decay in flight favors the transfer of most of the pion energy to the muon, since its mass is comparable to that of the pion. On the contrary, in the corresponding kaon decay the energy is equally distributed between the muons and the neutrinos. This means that kaons become the dominant source of neutrinos above ~100 GeV. On the other hand, muons are always dominated by pion decay, although the relative kaon contribution increases with energy. As mentioned earlier, due to the higher critical energy of kaons than pions, the kaon term in Eq. 1 reaches the asymptotic regime at higher energy than the pion term, making it relatively less sensitive to temperature variations [9]. Therefore the kaon-dominated neutrinos have a smaller correlation with temperature than muons [7].

5 Conclusions

Using neutrino-induced muon events reconstructed and selected with three years of IceCube data from April 2008 and May 2011, a seasonal variation in the neutrino event rate is observed for the first time. The neutrino rate for events in the horizontal region of $90^\circ < \theta < 120^\circ$ is observed to correlate with the effective temperature in the Earth's atmosphere in a manner that is consistent with studies of downward atmospheric muons performed with a much larger statistical data sample. Because of the importance of the kaon channel for production of muon neutrinos, further studies can contribute to understanding the kaon/pion ratio in the atmospheric cascade.

6 Acknowledgements

The temperature data used in this study were acquired as part of the NASA's Earth-Sun System Division and archived and distributed by the Goddard Earth Sciences (GES) Data and Information Services Center (DISC) Distributed Active Archive Center (DAAC).

References

[1] P.H. Barret *et al.*, Rev. Mod. Phys. 24 (1952) 133.
[2] M. Ambrosio *et al.*, Astrop. Phys. 7 (1997) 109.
[3] A. Bouchta, Proc. of 26th ICRC (1999) Salt Lake City, UT, U.S.A.
[4] M. Selvi, Proc. of 31st ICRC (2009) Łòdż, Poland.
[5] E.W. Grashorn *et al.*, Astrop. Phys. 33 (2010) 140.
[6] S. Tilav *et al.*, Proc. of 31st ICRC (2009) Łòdż, Poland, arXiv:1001.0776.
[7] P. Desiati *et al.*, Proc. of 32nd ICRC (2011) Beijing, China, arXiv:1111.2735.
[8] P. Adamson *et al.*, Phys.Rev. D81 (2001) 01200.
[9] P. Desiati and T.K. Gaisser, Phys. Rev. Lett. 105 (2010) 121102.
[10] M. Ackermann, E. Bernardini *et al.*, Proc. of 29th ICRC (2005) Pune, India, arXiv:astro-ph/0509330.
[11] S. Klein *et al.*, IceCube summary talk, these proceedings.
[12] R. Abbasi *et al.*, Phys. Rev. D 84 (2011) 082001.
[13] A. Schukraft *et al.*, Proc. of the 32nd ICRC (2011) Beijing, China, arXiv:1111.2736.
[14] J.A. Aguilar-Sanchez *et al.*, Proc. of NOW (2013) 10.1016/j.nuclphysbps.2013.05.029.
[15] http://disc.sci.gsfc.nasa.gov/AIRS/data-holdings.